Journal of Great Lakes Research 45 (2019) 277–289

Contents lists available at ScienceDirect

Journal of Great Lakes Research

journal homepage: www.elsevier.com/locate/jglr

Cyanobacterial blooms in the central basin of Lake Erie: Potentials for cyanotoxins and environmental drivers

Justin D. Chaffin [a,*], Sachidananda Mishra [b,e], Douglas D. Kane [a,c], Darren L. Bade [a,d], Keara Stanislawczyk [a], Kristen N. Slodysko [a,1], Kevin W. Jones [a], Eric M. Parker [a,2], Erica L. Fox [a]

[a] F.T Stone Laboratory, The Ohio State University and Ohio Sea Grant, 878 Bayview Ave. Put-in-Bay, OH 43456, United States of America
[b] Consolidated Safety Services Inc., Fairfax, VA, United States of America
[c] Division of Natural Science, Applied Science, and Mathematics, Defiance College, Defiance, OH, United States of America
[d] Department of Biology, Kent State University, Kent, OH, United States of America
[e] National Centers for Coastal Ocean Science, National Ocean Service, National Oceanic Atmospheric Administration, Silver Spring, MD, United States of America

ARTICLE INFO

Article history:
Received 25 June 2018
Accepted 3 December 2018
Available online 11 January 2019

Communicated by Robert Michael McKay

Keywords:
Anabaena
Dolichospermum
Eutrophication
Microcystis
Saxitoxins
Water quality

ABSTRACT

Lake Erie western basin (WB) cyanobacterial blooms are a yearly summer occurrence; however, blooms have also been reported in the offshore waters of the central basin (CB), and very little is known about what drives these blooms or their potential for cyanobacterial toxins. Cyanobacteria Index was quantified using MODIS and MERIS data for the CB between 2003 and 2017, and water samples were collected between 2013 and 2017. The goals were to 1) quantify cyanobacteria, 2) determine environmental drivers of CB blooms, and 3) determine the potential for cyanobacterial toxins in the CB. *Dolichospermum* (*Anabaena*) occurred in the CB during July before the onset of the WB bloom, and then in August and September, the cyanobacteria community shifted towards *Microcystis*. The largest *Dolichospermum* blooms (2003, 2012, 2013, and 2015) were associated with reduced water clarity (Secchi disk depth < 4 m), whereas large CB *Microcystis* blooms (2011 and 2015) were associated with large WB blooms. *Dolichospermum* blooms occurred in high nitrate concentrations (>20 μmol/L) and high nitrogen-to-phosphorus ratios (>100), which indicate nutrient concentrations or ratios did not select for *Dolichospermum*. Additionally, the *sxtA* gene, but not *mcyE* or microcystins, were detected in the CB during July 2016 and 2017. The *mcyE* gene and microcystins were detected in the CB during August 2016 and 2017. The results indicate the CB's potential for cyanotoxins shifts from saxitoxins to microcystins throughout the summer. Continued monitoring of cyanobacteria and multiple cyanobacterial toxins is recommended to ensure safe drinking water for CB coastal communities.

Introduction

Lake Erie (USA and Canada) underwent eutrophication during the mid-1900s as a consequence of excessive nutrient loading (Chapra and Robertson, 1977). Total phytoplankton biomass increased throughout the 20th century, and cyanobacterial blooms were an annual summer occurrence (Davis, 1964; Snodgrass, 1987). To combat eutrophication, the governments of Canada and USA enacted the Great Lakes Water Quality Agreement (GLWQA) which required phosphorus (P) load reductions (Matisoff and Ciborowski, 2005). The water quality of Lake Erie rapidly improved due to these regulations, resulting in decreased total P concentrations (DePinto et al., 1986), lower phytoplankton and cyanobacterial biomass (Makarewicz, 1993), higher hypolimnetic dissolved oxygen concentrations and fewer fish kills (Ludsin et al., 2001). However, since the mid-1990s, Lake Erie has once again experienced eutrophication (Conroy et al., 2005; Kane et al., 2014; Scavia et al., 2014; Watson et al., 2016).

Lake Erie, Earth's 15th largest lake by volume (489 km^3) and 10th by surface area (25,700 km^2), is regarded to have three basins with different bathymetry, chemical, and biological characteristics (Bolsenga and Herdendorf, 1993; Herdendorf, 1982). The western basin accounts for about 10% of the lake's surface area, is the shallowest basin (average depth of 8 m), has the warmest water temperatures during the summer, and usually does not thermally stratify (Bridgeman et al., 2006). Furthermore, the western basin has been designated impaired by the states of Michigan and Ohio due to annual cyanobacterial blooms (Davis et al., 2019). The central basin has an average depth of 22 m and has meso- to oligotrophic status. A thin hypolimnion (<5 m) forms every summer that is prone to anoxic conditions by mid to late-summer (Scavia

* Corresponding author.
E-mail address: Chaffin.46@osu.edu (J.D. Chaffin).
[1] Present address: Department of Environmental Science, State University of New York College of Environmental Science and Forestry. Syracuse, NY.
[2] Present address: Department of Biology, Central Michigan University, Mount Pleasant, MI.

https://doi.org/10.1016/j.jglr.2018.12.006
0380-1330/

et al., 2014; Zhou et al., 2013). The eastern basin has the coolest summertime temperature, is the deepest area of the lake, and has the least amount of offshore phytoplankton.

Cyanobacterial blooms in Lake Erie's western basin are capable of producing high concentrations of microcystins, which are a group of >100 similar toxins produced by a large number of cyanobacterial genera (Gobler et al., 2016). In August 2014, a "do not drink" advisory was issued for the city of Toledo, Ohio because microcystins were detected in drinking water at levels above the World Health Organization's guideline of 1 μg/L (Qian et al., 2015; Steffen et al., 2017). The non-nitrogen (N) fixing genera *Microcystis* dominates the blooms, and the annual biomass of cyanobacteria in the western basin is highly correlated with springtime total bioavailable phosphorus (P) loading from the Maumee River, which allows for seasonal forecasts of bloom severity (Stumpf et al., 2016). However, Lake Erie is not only prone to *Microcystis* blooms in the western basin. Sandusky Bay has dense blooms of filamentous, non-N-fixing, *Planktothrix* every year, and bloom biomass is not correlated with nutrient loading (Conroy et al., 2017; Davis et al., 2015). Additionally, *Lyngbya wollei* is a filamentous benthic cyanobacterium that grows attached to the sediments in the nearshore zones of the western basin and can accumulate in high biomasses along the lake shore (Bridgeman and Penamon, 2010). Cyanobacterial blooms in the central basin are also often detected by satellites, and Wynne and Stumpf (2015) showed that satellite-detectable cyanobacterial biomasses were present about 20% of the time in the offshore waters between July 1 and July 20 for years 2002–2014. Additionally, large blooms of *Microcystis* in the western basin (e.g., 2011 and 2015) can be spread via water currents into the central basin in late summer (Chaffin et al., 2014). Information about the central basin phytoplankton community assemblages is currently restricted to monitoring cruises conducted by US EPA in April and August (Reavie et al., 2014). These data show an increase of cyanobacteria biovolume in Augusts between 2001 and 2011 (Reavie et al., 2014); however, the US EPA cruises miss the July blooms detected by satellites. Additionally, Scavia et al. (2014) reported an increase of total phytoplankton biomass, total P concentrations, decreased water transparency, and an increase in the areal extent of hypoxia (DO <2.0 mg/L) between 1996 and 2011 in the central basin, indicating re-eutrophication of the basin.

While excess P loading has been a known driver of eutrophication and cyanobacterial blooms (Schindler, 1977), there are other important factors. Nitrogen (N) has been shown to constrain cyanobacterial biomass, and many researchers have called for dual nutrient management (P and N) to mitigate eutrophication and blooms (Conley et al., 2009; Lewis and Wurtsbaugh, 2008); however, there is continued debate over dual nutrient management (Paerl et al., 2016b; Schindler et al., 2016). The non-N-fixing cyanobacterium *Microcystis* can persist in low N waters due to its highly competitive nature for ammonium that is regenerated from the decomposition of organic matter (Blomqvist et al., 1994; Paerl et al., 2011). Diazotrophic (N-fixing) cyanobacteria, such as *Dolichospermum* (formally, *Anabaena*) and *Aphanizomenon*, are favored in N-poor, P-rich waters due to their ability to use atmospheric dinitrogen gas (Smith, 1983), although several exceptions to this generality have been noted (Paerl and Otten, 2016). Nitrate assimilation and N-fixation are dependent on iron (Fe) and molybdenum (Mo) cofactors (Flores and Herrero, 2005). Large colony-forming cyanobacteria have a competitive advantage over eukaryotic phytoplankton in waters with low Fe availability due to their ability to use Fe-scavenging siderophores to access reduced Fe^{2+} in anoxic bottom waters (Molot et al., 2014; Sorichetti et al., 2016; Verschoor et al., 2017). Buoyancy regulation of surface scum-forming cyanobacteria (i.e., *Microcystis*, *Dolichospermum*, *Aphanizomenon*) provides a competitive advantage over negatively or neutrally buoyant eukaryotic phytoplankton in light-limited waters (Huisman et al., 2004; Reynolds et al., 1987). Cyanobacteria have higher optimum growth temperatures than eukaryotic phytoplankton, and warm waters may select for cyanobacteria (Paerl et al., 2016a; Paerl and Huisman, 2008). Because the central basin of Lake Erie has lower nutrient (P and N) concentrations than the western basin, it is expected that these other environmental factors have a role in early summer cyanobacterial blooms of the central basin (Fig. 1).

The purpose of this research was to: 1) identify and quantify the early summer central basin cyanobacterial blooms, 2) determine likely environmental drivers of the central basin blooms including nutrient concentrations, water temperature, water clarity, and hypolimnetic DO concentrations, and 3) determine potential for cyanobacterial toxins (microcystins, saxitoxins, and cylindrospermospins) of the blooms. While western basin *Microcystis* blooms have been documented to spread into the central basin in late summer (September and October; Chaffin et al., 2014), the primary focus of this study was the central basin blooms that occur during early summer (June and July).

Methods

Satellite data

MEdium Resolution Imaging Spectrometer (MERIS) L2 data for the years 2003–2011 and Moderate Resolution Imaging Spectroradiometer (MODIS) Aqua L2B data for the years 2012–2017, with a nominal 1 × 1 km pixel resolution, were downloaded from NASA ocean color website. Both time series were restricted to June through September each year to focus only on the early summer (June and July) bloom and a subsequent equivalent amount of time in late summer (August and September). Data were processed using NOAA's satellite automated processing system (SAPS), which incorporates l2gen available in NASA's SeaDAS 7.1. Images are projected to UTM projection with nearest neighbor interpolation with the l2gen Rayleigh corrected reflectance (ρ_s) product as the primary output. Clouds and mixed pixels affected by land adjacency were detected and flagged following the methods in Stumpf et al. (2012).

Cyanobacterial algorithm

For MERIS, Cyanobacteria Index (CI) was calculated using a spectral shape (SS) of ρ_s around 681 nm, which relates to chlorophyll (chl) *a* absorption in cyanobacteria at 681 nm (Wynne et al., 2008). Apparent reflectance generated from fluorescence by eukaryotes at 681 nm obscures the non-cyanobacterial chl *a* pigment absorption signal, which helps CI to discriminate cyanobacteria from eukaryotes effectively. In addition, a spectral shape using 620, 665, and 681 nm was used to identify the presence of phycocyanin (Lunetta et al., 2015), which is a characteristic photo-pigment in cyanobacteria, and a positive value of the spectral shape indicated the presence of phycocyanin. For the MODIS dataset, the spectral shape was adjusted using available 667, 678, and 748 nm MODIS bands for detection of cyanobacteria (Wynne et al., 2013; Wynne and Stumpf, 2015). Finally, the mean CI of the central basin for each MERIS and MODIS image was calculated for the entire time series (2003–2017) using GDAL (GDAL/OGR contributors, 2018). A few left out land-contaminated mixed pixels erroneously affected mean CI values as the central basin mean CI is very low. In order to avoid the mixed pixels and nearshore localized blooms, a 5 km inward buffer from the shoreline was used to extract basin scale zonal means for each available date in the entire time series.

Sample collection & handling methods

Data and water sample collection occurred at 4 locations within the central basin (Fig. 1) beginning in summer 2013, with the primary focus of collecting water profiles of dissolved oxygen (DO) and nutrient concentration. In 2014, we began collecting phytoplankton at each site, in addition to DO and nutrients, and then sample frequency was increased during 2016 and 2017. Additionally, we collected "event" based samples when cyanobacterial blooms were reported (by NOAA HAB Bulletins, local agencies, or local media) in areas of the central basin both outside of our sampling locations or when blooms occurred when sampling was

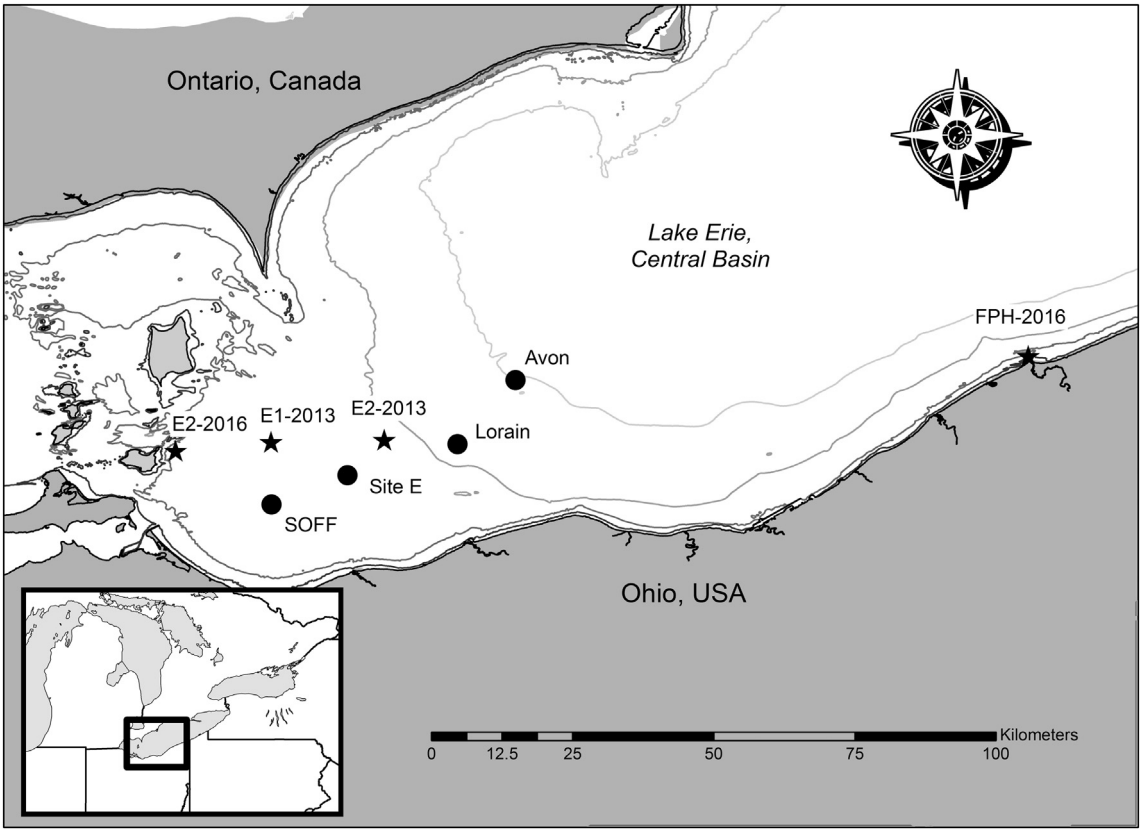

Fig. 1. Map of sample locations in the central basin of Lake Erie. The four fixed-sample locations are represented by black circles and the bloom event samples are black stars.

not scheduled. Sampling conducted within the sampling area was collected aboard the R/V Erie Monitor or R/V Gibraltar III, whereas event-based samples outside of the area were collected from small motorboats owned by local agencies or groups.

Upon arriving on station location, the anchor was deployed and time and date of sample, site depth, weather conditions, Secchi disk depth, and GPS coordinates were recorded. Vertical profiles of DO (mg/L) and water temperature (°C) were recorded at 0.5-m intervals throughout the water column to within 15 cm of the lake bottom with a Yellow Springs Instruments (YSI) multiprobe sonde 6600v2 in years 2013–2015 and with a YSI EXOv2 in 2016 and 2017. All sample bottles used in this research were acid washed (1.2 N HCl and rinsed with deionized water) before sample collection. Immediately before sample collection, sample bottles and water collection equipment were triple rinsed with lake surface water. Epilimnetic water samples were collected with an 8-m-long integrated tube sampler and deposited into a clean, lake-rinsed 18.9-L bucket (Golnick et al., 2016), which was repeated 5 times per station and the water pooled together. The YSI temperature profile confirmed that the hypolimnion was below 8 m from the surface. Water intended for chl *a* analysis was poured into a 2-L dark polyethylene bottle. Water intended for total phosphorus (TP) and total Kjeldahl nitrogen (TKN) analysis was poured into separate 250 mL bottles. Water for phytoplankton enumeration was poured into 0.5-L or 1.0-L glass bottles, preserved with Lugol's solution (1%), and kept dark. Water for dissolved nutrient (nitrate, nitrite, ammonium, dissolved reactive P, and silicate) analysis was filtered upon collection with a 0.45-μm membrane syringe filter. The syringe was rinsed 3 times with surface water and the 60-mL polyethylene bottle was rinsed 3 times with 10–15 mL of filtered sample (unfiltered lake water was not used as a rinse). Water for total microcystins concentration was poured into 40-mL amber glass vials. All samples were held on ice while in transport back to the laboratory. The above sample collection methods were conducted every year of the study.

Additional water samples were collected in 2016 and 2017. A metal-free 4-L vertical Kemmerer sampler was used to sample water from 1.5 m depth, and the samples were field filtered with a 0.45 μm membrane syringe filter for analysis of total dissolved Fe and Mo. To determine the potential cyanotoxins of the central basin blooms, water from the integrated sampler was used to fill 1-L polyethylene terephthalate-glycol (PETG) bottles for analysis of total cyanobacteria gene copies and cyanotoxin genes (microcystins, saxitoxins, and cylindrospermopsins). Finally, to determine if the onset of anoxia (DO < 0.1 mg/L) and sediment-released nutrients correlated with bloom formation, on one date in 2016 and all dates in 2017, hypolimnion water samples were collected with the Kemmerer 0.5 m above the lake bottom for total and dissolved nutrient and total dissolved Fe and Mo. All samples were held on ice until processing occurred. Table 1 summarizes the parameters that were tested for each year.

Upon arriving back to the laboratory, all nutrient and total microcystins samples were stored at −20 °C until analysis. Plankton from the 2-L bottle were filtered (500 to 1000 mL) on to a GF/F filter, noting the volume filtered, and stored at −80 °C on silica gel for analysis of chl *a* concentration. The Lugol's preserved phytoplankton samples were poured into a 1-L graduated cylinder, the exact volume was recorded, and allowed to settle for 2 days in the dark. After 2 days, the sample was siphoned down to ~50 mL, poured into 50 mL graduated cylinder to resettle for 2 days, siphoned down to 15 mL; and then the sample stored in an amber glass vial. Water (100 to 500 mL) for genetic analysis of the cyanobacteria was filtered onto 2.0 μm polycarbonate filters and stored at −80 °C in 2 mL microfuge tube.

Laboratory analysis

Table 1 summarizes the analytical methods used for each parameter. Chl *a* from GF/F filters was extracted with dimethyl sulfoxide and quantified via spectrophotometry (Golnick et al., 2016; Wellburn, 1994). A

Table 1
Parameters analyzed, the methods used, method detection limits and units, and the years in which the data was collected. The abbreviations are defined in the text.

Parameter		Analytical method	MDL and units	2013	2014	2015	2016	2017
Chl *a*	Filter extracted	Golnick et al., 2016	0.5 μg/L	Partly	Yes	Yes	Yes	Yes
TP	Unfiltered	EPA 365.3	0.05 μM	Yes	Yes	Yes	Yes	Yes
TKN	Unfiltered	EPA 351.2	1.44 μM	No	Yes	Yes	Yes	Yes
Nitrate	Filtered	EPA 353.1	0.17 μM	Yes	Yes	Yes	Yes	Yes
Nitrite	Filtered	EPA 354.1	0.04 μM	Yes	Yes	Yes	Yes	Yes
Ammonium	Filtered	EPA 350.1	0.55 μM	Yes	Yes	Yes	Yes	Yes
DRP	Filtered	EPA 365.1	0.04 μM	Yes	Yes	Yes	Yes	Yes
Silicate	Filtered	SEAL 027–04	0.48 μM	Yes	Yes	Yes	Yes	Yes
Total microcystins	Unfiltered	Abraxis ELISA	0.10 μg/L	Yes	Yes	Yes	Yes	Yes
Phytoplankton	Unfiltered	FlowCam	NA	Yes	Yes	Yes	Yes	Yes
TDFe	Filtered	ICP-MS	5.0 nM	No	No	No	Yes	Yes
Cyanobacteria 16S rRNA	Filter extracted	qPCR	1–5 gene copies/mL	No	No	No	Yes	Yes
mcyE, sxtA, cyrA	Filter extracted	qPCR	1–5 gene copies/mL	No	No	No	Yes	Yes

continuous segmented flow auto-analyzer (QuAAtro SEAL Analytical Inc., Mequon, WI) was used to quantify nitrate, nitrite, ammonium, dissolved reactive P, and silicate using standard U.S. EPA methods (Table 1). Seven known concentration standard solutions (including 0) were used for the standard curve ($R^2 > 0.999$), and every-tenth sample was spiked with a known amount of analyte to ensure high accuracy and precision throughout the analysis (>95% recovery). Total P (TP) was determined with unfiltered water following a sulfuric acid/persulfate digestion and autoclaved at 121 °C for 45 min. Total Kjeldahl N (TKN) was determined on the unfiltered water with a sulfuric acid/copper sulfate digestion with a block digester for 60 min at 180 °C then 120 min at 380 °C. Total P and TKN were then quantified on the SEAL QuAAtro analyzer. Total N was calculated as the sum of TKN, nitrate, and nitrite, and the TN to TP (TN: TP) ratio was calculated by dividing TN by TP. Total dissolved Fe and Mo samples were prepared at 2.0% nitric acid for analysis in ICP-MS (Xseries 2, Thermo Scientific, MA, USA). For quantitative analysis, standards and internal standards were prepared by using the certified ICP-MS standards from Inorganic Ventures. Correlation coefficients for calibration curves were above 0.999. ICP-MS was conducted at the Center for Metals at the University of Toledo.

Phytoplankton from the Lugol's concentrated samples were identified and quantified with a FlowCAM (Fluid Imaging Technologies, Inc.) following the methods listed by Chaffin et al. (2018). FlowCAM areal measurements were used as surrogates for cell counts. Cyanobacteria biovolume was calculated from FlowCAM areal measurement (Chaffin et al., 2018).

To determine total microcystins, the samples were subjected to 3 freeze/thaw cycles, filtered with GMF (0.45 μm pore size) to remove cellular debris, and quantified using enzyme-linked immunosorbent assay (ELISA) (Abraxis #520011). The method detection limit for total microcystins was 0.10 μg/L. According to the manufacturer's guidelines, the microcystins ELISA has good cross-reactivity with various congeners of microcystins.

Multiplex quantitative PCR (qPCR) was used to quantify gene copies of the 16s rRNA gene, which is an indicator of total cyanobacteria, and the *mcyE*, *sxtA*, and *cyrA* genes, which are required for microcystins, saxitoxins, and cylindrospermopsins production, respectively (Al-Tebrineh et al., 2012). Phytoxigene™ CyanoDTec cyanobacteria-specific primers were used, rather than genera or species-specific primers, in order to provide insights into potential bloom toxins without concern for which cyanobacteria genera would be responsible for toxins. qPCR was conducted at the Northeast Ohio Regional Sewer District following methods and cycles listed in the Ohio EPA method 705.0. Method detection limits ranged from 1 to 5 gene copies/mL depending on the volume of water filtered.

Data analysis

The satellite CI data was handled similarly as Stumpf et al. (2012). All pixels with detected CI in each daily cloud-free image were averaged to estimate the basin-wide mean cyanobacteria biomass. The highest basin-wide CI average over 10-day time frames (first of each month to the 10th day, 11–20, and 21 to 30 or 31) was selected to estimate cyanobacterial biomass for each time frame. Then, the CIs of the six time frames in June and July were summed together and the six time frames in August and September were summed to quantify early summer and late summer blooms separately.

Because we were more interested in the early summer cyanobacterial blooms, the physical and chemical data collected between 1 June and 31 July was subject to a 2-factor ANOVA with site and year as factors to determine if the data could explain bloom patterns among the 5-year study.

Results

Satellite data

MERIS and MODIS detected varying levels of cyanobacterial biomass in the central basin during June and July every summer since 2003 (Figs. 2 and 3). 2013 had the largest peak in biomass, whereas 2008 and 2017 had the lowest peak biomass. The peak biomass for each year occurred during a three-week window between 27 June and 20 July (Fig. 2A). 2013 and 2015 had greatest cumulative June and July biomass (Fig. 2B). There was no apparent temporal pattern of cumulative June and July biomass.

During August and September 2003 to 2007 had very low cumulative cyanobacterial biomass, but cumulative biomass has increased since 2008 (Fig. 2B). August and September of 2011 and 2015 had the highest cumulative biomass, which were summers with large western basin *Microcystis* blooms (Stumpf et al., 2016). In the earlier years, the June and July cumulative biomass exceeded biomass in August and September, but that pattern has reversed in the more recent years.

Phytoplankton community and biomass

Dolichospermum (formally *Anabaena*) was the dominant cyanobacterial genera in the central basin each year since 2013 in June and July, with the greatest *Dolichospermum* biovolume during July (Figs. 4 and 5), and several *Dolichospermum* species were identified, including *D. lemmermannii, D. circinale,* and *D. planctonicum* (quantification was carried out at the genus level). The highest biovolumes of *Dolichospermum* were found during the bloom event samples collected in 2013. Biovolumes of *Dolichospermum* were lower during August and September, or *Dolichospermum* was not detected. Therefore, the peaks of CI since 2013 in June and July corresponded to *Dolichospermum* dominance. One surface scum sample collected by a local fisherman off of Avon Lake, Ohio during July 2007 was identified as *Dolichospermum* (Chaffin, personal observation).

Microcystis and *Aphanacapsa* were the dominant cyanobacteria in August and September; however, due to difficulties in differentiating

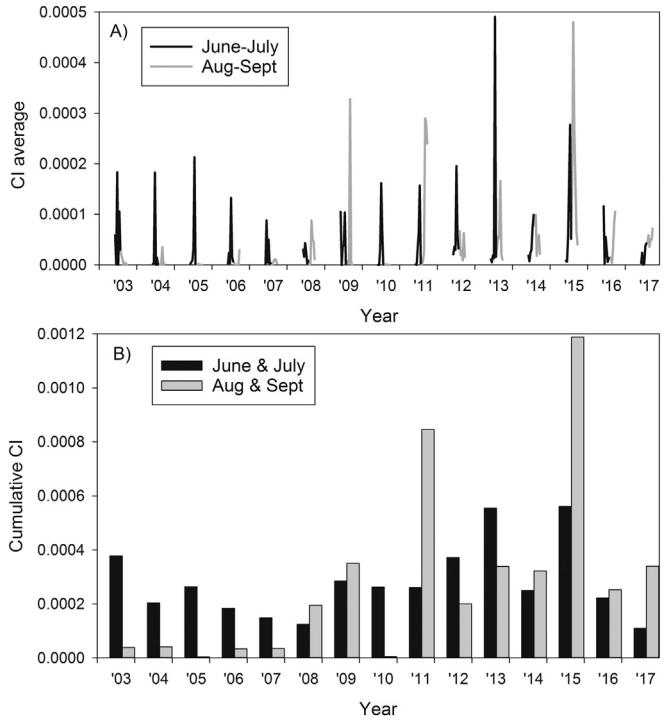

Fig. 2. (A) Time series of central basin cyanobacterial index (CI) average for years 2003–2017, and (B) the cumulative sum of the six 10-day time frames during 1 June to 31 July and 1 August to 31 September.

some *Microcystis* colonies from *Aphanacapsa* colonies in the Lugol's preserved samples using the FlowCAM, both genera were grouped into *Microcystis* for this report (as in Reavie et al., 2014). *Microcystis* was in low biovolumes or not present during June and July, and reached its highest biovolumes in August and September. Peaks of CI since 2013 in August and September corresponded to *Microcystis* dominance.

Less abundant cyanobacterial genera were also present. Planktonic *Lyngbya* was present in late July, August, and September of 2016 and 2017 (Fig. 5). *Planktothrix* was also present in most samples but at lower biovolumes, and the highest biovolumes of *Planktothrix* were recorded during the bloom event samples collected in 2013 (Fig. 4). Other cyanobacterial genera including *Aphanizomenon*, *Merismopedia*, *Woronichinia*, and *Snowella* were present, but their biovolumes made up <1% of the total cyanobacteria biovolume and not included in the figures.

The overall phytoplankton community of the central basin was very diverse (Fig. 4). The chain-forming diatom *Fragilaria crotonensis* and chrysophyte *Dinobryon* were common in most samples. Cryptomonads and several genera of green algae were also present. Chl *a* concentrations ranged from 0.64 μg/L to 15.28 μg/L during June and July and the chl *a* range increased to 2.86 to 28.08 μg/L for August and September (Electronic Supplementary Material (ESM) Fig. S1).

Cyanobacterial toxins

Microcystins were only detected on one date during the June and July (15 July 2013) period at concentrations of 1.71 and 1.18 μg/L on an event-based sampling trip (ESM Fig. S2), and both *Dolichospermum* and *Planktothrix* were present on that date (Fig. 4). Microcystins were detected in August and September of 2014, 2015, and 2016 when *Microcystis* was present. Total microcystins concentrations ranged from below detectable levels (<0.1 μg/L) to 2.1 μg/L with the highest concentrations measured in August 2015.

Cyanotoxin gene copies detected by qPCR are presented in Fig. 6. The *mcyE* gene was only detected on two of the nine July 2016 samples (both 5 copies/mL) and just one July 2017 sample (148 copies/mL) (Fig. 6b). The gene *mcyE* was detected in two of the three August 2016 samples (578 and 715 copies/mL) and in all three August 2017 samples (13 to 134 copies/mL). The *sxtA* gene was detected in all nine July 2016 samples (range 1 to 304 gene copies/mL) and three of the nine July 2017 samples (range 19 to 64 copies/mL) (Fig. 6c), but *sxtA* was not detected in August of either year (3 samples in August of each year). The cylindrospermopsin gene, *cyrA*, was not detected in any sample.

Physical and chemical properties

Surface water temperature did not significantly differ ($p = 0.679$) among years and sites. In general, at all locations and during every summer, surface water temperature increased throughout June and July, reached warmest temperatures in late July or early August, and then began to decrease (Fig. 7, top row). Water temperatures measured just above the sediments (15 cm above sediments) were 5 °C to 17 °C colder than surface water, which indicates stratification, and bottom temperatures increased throughout summer (Fig. 7, top row). Mixing events (as indicated by same surface and bottom temperatures) frequently occurred during 2013 at site SOFF, 2015 at sites E and SOFF, and during late July and August in 2017. The deeper sites, Avon and Lorain, had significantly ($p < 0.001$) cooler bottom water temperatures than the shallower sites, E and SOFF.

Dissolved oxygen measured just above the sediments ranged from <0.1 mg/L to 8.86 mg/L (Fig. 7, middle row), and there was no significant difference among sites and years ($p = 0.307$). Hypolimnion DO concentrations decreased throughout summer, but there were notable instances when DO levels increased as the result of mixing.

Secchi disk depths ranged from 0.96 to 10.40 m (Fig. 7 bottom row), and there were significant differences in the Secchi disk depth among years ($p < 0.001$) and among sites ($p < 0.001$; no interaction $p = 0.440$). The average Secchi disk depths in 2013 and 2015 were lower than years 2014, 2016, and 2017, and the average Secchi disk depth increased from west to east.

Epilimnetic nitrate concentrations ranged from 6.42 to 54.68 μmol/L (Fig. 8 top row) and significantly differed among sites ($p = 0.026$) and years ($p < 0.001$). Nitrate concentrations decreased west to east, but no apparent pattern was recognizable over the years. Nitrate concentrations displayed a seasonal pattern every year with the highest concentrations recorded in late June, which then decreased throughout the summer season. Total phosphorus concentrations ranged from 0.085 to 0.670 μmol/L (Fig. 8, second row), and did not significantly ($p = 0.057$) differ among years and sites. Total nitrogen concentrations ranged from 24.6 to 81.9 μmol/L (not shown) and differed significantly among sites ($p = 0.016$) but not among years. Similar to nitrate concentration, total nitrogen concentration decreased west to east. The TN: TP ratio ranged from 59.0 to 640.7 (molar ratio) and did not significantly ($p = 0.077$) differ among years and sites. TN: TP followed the same seasonal pattern as nitrate concentration. Finally, silicate concentrations ranged from 0.86 to 24.60 μmol/L (Fig. 8, bottom row) and significantly differed among years ($p < 0.001$) but not by sites ($p = 0.121$). Silicate concentrations were extremely variable in 2013, 2014, and 2015, whereas, in 2016 and 2017 silicate concentrations followed the same temporal pattern at all sites. Epilimnion ammonium and DRP were below detectable concentrations in all samples.

Total dissolved Fe in the epilimnion was below detection (<5 nM) in all 2016 and 2017 samples. The samples were also analyzed for total dissolved Mo, but Mo was detected in field blanks at concentrations above the method detection limit. Therefore, Mo data was rendered invalid due to potential contamination.

Hypolimnetic total dissolved Fe concentrations at sites Avon and Lorain on 2016 August 26 were 10.45 and 8.52 μmol/L, respectively (ESM Fig. S4), and the water was anoxic (DO was <0.1 mg/L). However, total dissolved Fe concentrations at Site E and SOFF on the same day were below detection, and DO was 0.4 mg/L. Likewise, the anoxic sites had DRP concentrations >2 μmol/L and ammonium >10 μmol/L, whereas

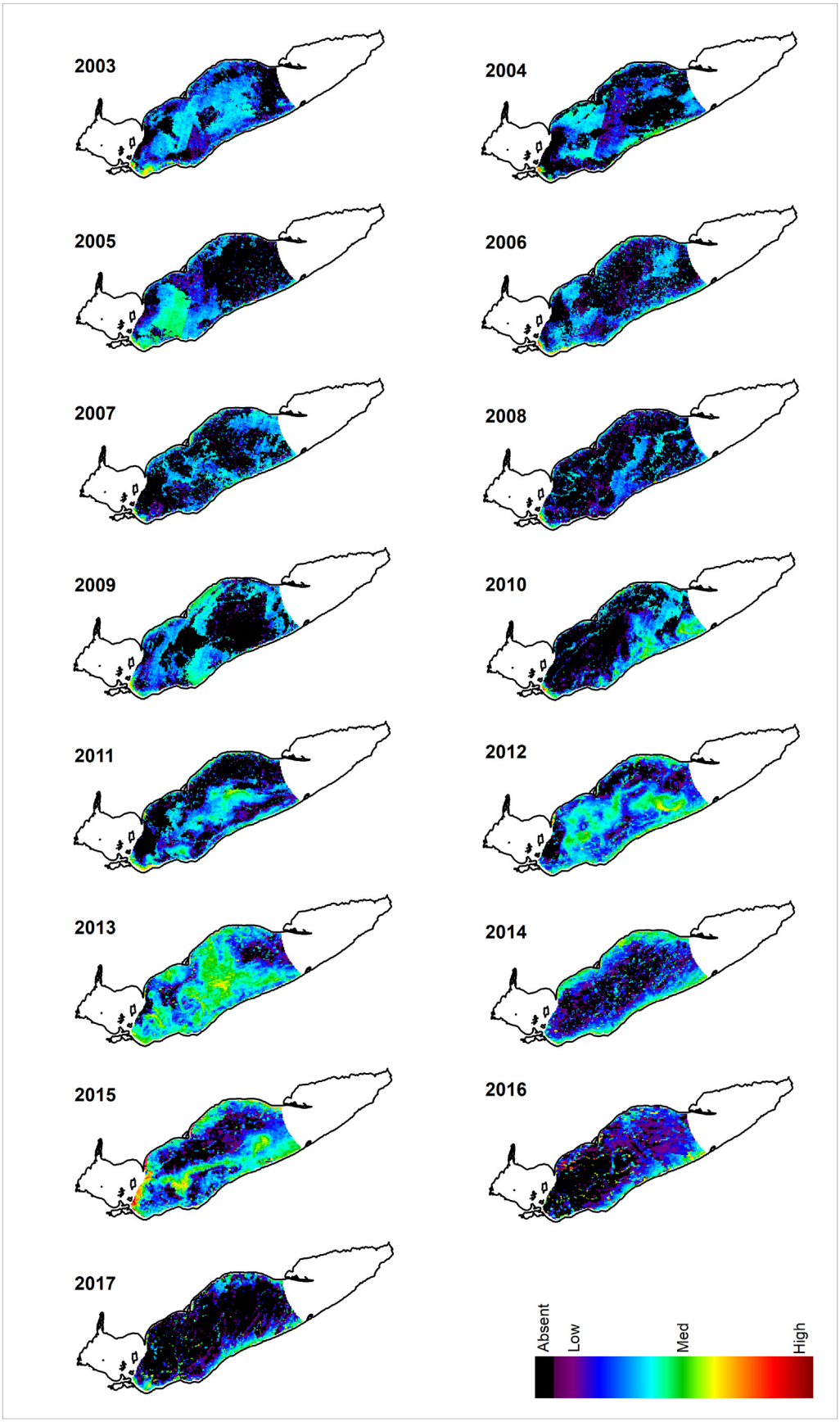

Fig. 3. Maximum cyanobacterial index in central basin during June and July 2003–2017.

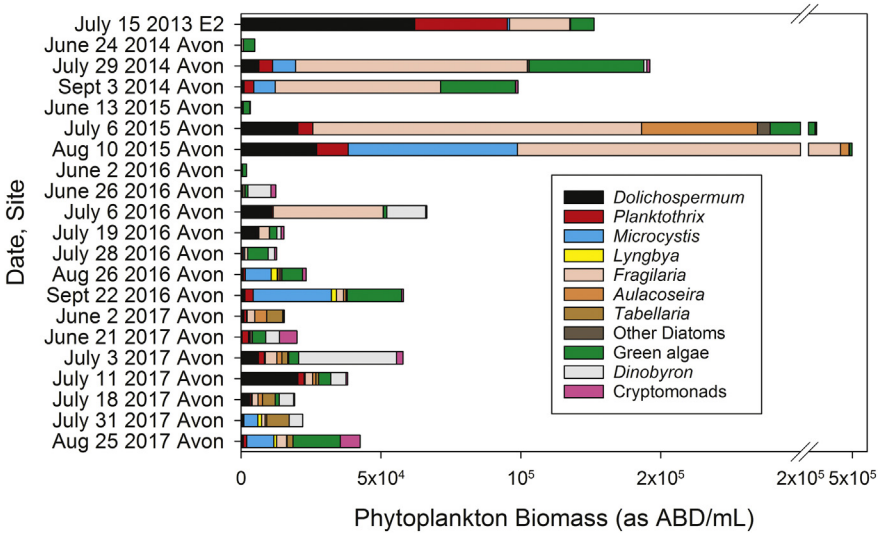

Fig. 4. Phytoplankton biomass at site Avon 2014–2017 and during a bloom event sample on 2013 July 15. Biomass was determined by a FlowCAM in the units of areal based diameter (ABD, μm^2/mL). The *Microcystis* category also includes *Aphanocapsa* due to difficulty in differentiating colonies in Lugol's preserved samples. The relationship between colony area and biovolume could not be determined for all taxa, hence, the data is presented as area per mL.

the oxic sites had DRP less than method detection limit and lower ammonium concentrations.

Total dissolved Fe and DRP were below detection in all hypolimnion samples in 2017 (ESM Fig. S4). Hypolimnion ammonium concentrations ranged from below detection to 11.02 μmol/L, and most samples had ammonium concentrations >2 μmol/L. Total P concentrations were similar between hypolimnion and epilimnion.

Discussion

Central basin cyanobacteria community composition

Cyanobacterial blooms were present in the central basin of Lake Erie every year since 2003 at varying biomasses (Fig. 2). Field sampling from 2013 to 2017 identified *Dolichospermum* as the dominant cyanobacterium in the central basin during June and July. Peaks in CI were present every year between 27 June and 20 July (except 2008), which is before the onset of the western basin *Microcystis* blooms. While the June and July blooms 2003–2012 cannot be identified due to lack of samples, one surface sample collected by a local fisherman in July 2007 offshore of Avon Lake, Ohio was identified as *Dolichospermum* (Chaffin, personal observation). Taken together, these results indicate that the July central basin blooms occurred independently of the western basin blooms. Furthermore, the CI (Fig. 3) and chl *a* concentrations (ESM Fig. S1) during the July *Dolichospermum* blooms in the central basin were much lower than concentrations reported for the western basin and Sandusky Bay, (Chaffin et al., 2013; Davis et al., 2015), which indicates lower cyanobacterial biomass in the central basin.

Microcystis was responsible for cyanobacterial blooms in the central basin in August and September. The years 2011 and 2015 had the largest cumulative cyanobacterial biomasses, and these years also had the two largest western basin *Microcystis* blooms in recent history (Stumpf et al., 2016) indicating that large western basin blooms spread eastward to the central basin. Molecular tracking of the 2011 bloom confirmed that the central basin *Microcystis* community structure during September and October was similar to the *Microcystis* community structure of the western basin during July and August (Chaffin et al., 2014). However, 2013 and 2017 also had large western basin blooms, but those blooms remained in the western basin.

The two largest *Dolichospermum* blooms occurred in the past five years, and there has been an increase of *Microcystis* biomass in the central basin during the last ten years. These results provide further

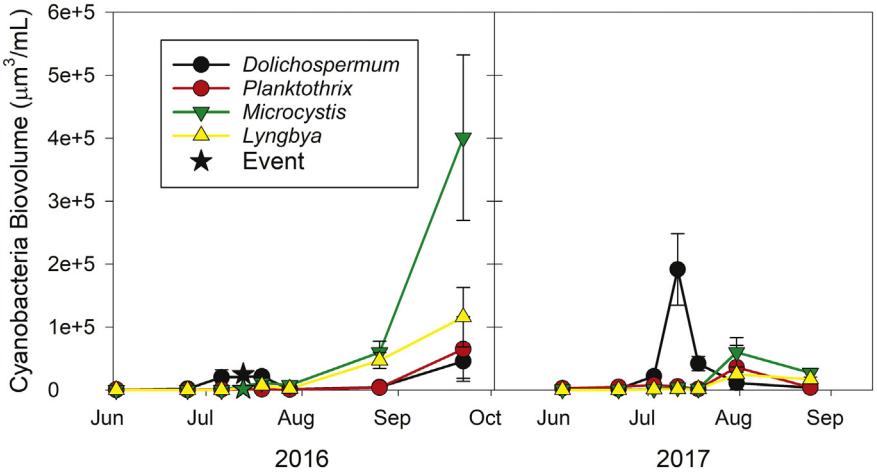

Fig. 5. Average cyanobacteria biovolume (μm^3/mL) (±1 S.E.) at 4 fixed-location sample sites in the central basin during 2016 and 2017. The stars indicate samples that were collected from the Fairport Harbor bloom on 2016 July 13. The *Microcystis* category also includes *Aphanocapsa* due to difficulty in differentiating colonies in Lugol's preserved samples.

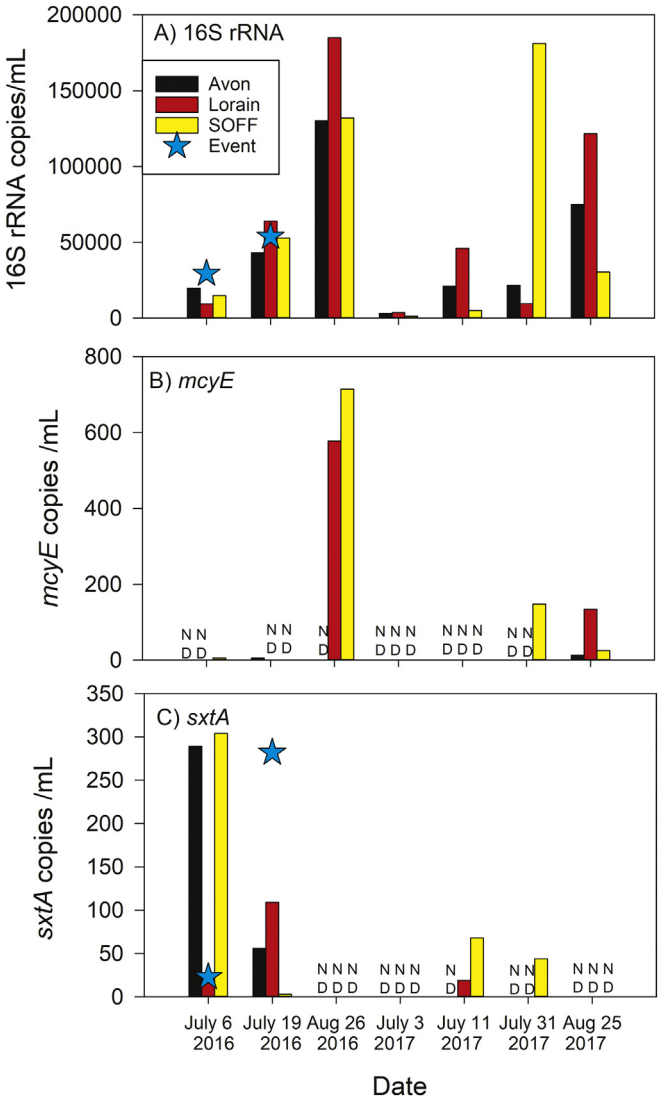

Fig. 6. Total cyanobacterial 16S rRNA (A), *mcyE* (B), and *sxtA* (C) gene copies measured at 3 fixed sites (bars) and event-based locations (stars). ND = not detected.

evidence of the degrading water quality of Lake Erie and that the symptoms of eutrophication observed in the western basin are now also occurring in the central basin, as suggested in Kane et al. (2015, 2014).

Environmental drivers of the Dolichospermum blooms

Water temperature is a primary regulatory factor in the formation of cyanobacterial blooms, and warmer temperatures favor cyanobacteria (Paerl et al., 2016a; Paerl and Huisman, 2008; Visser et al., 2016). Central basin surface water temperatures ranged from 16.0 °C to 25.8 °C during the June–July periods in this study (Fig. 7) and did not significantly differ among years. Water temperatures in June and early July (16–22 °C) align more closely with the optimal growth temperatures reported for several species of *Dolichospermum* (Zapomělová et al., 2010), and Capelli et al. (2017) suggested that *Dolichospermum lemmermannii* can adapt to temperature variations. Also, the early July temperatures were not high enough to inhibit eukaryotic phytoplankton growth (Paerl et al., 2016a), hence the highly diverse phytoplankton community (Fig. 4). Whereas, the water temperatures in August (upper 20s°C) align more closely with *Microcystis* optimal growth temperatures (O'Neil et al., 2012; Paerl and Otten, 2016). The increase in water temperature throughout summer could, at least in part, explain the *Dolichospermum* to *Microcystis* succession pattern. However, allelopathic interactions between *Dolichospermum* and *Microcystis* could also play a role in the succession pattern observed in the central basin, because *Microcystis* reduced *Dolichospermum* growth in culture experiments (Chia et al., 2018).

The water temperature data during the five years of sample collection did not differ among year and site, which suggests temperature did not impact the size of the *Dolichospermum* blooms. However, the average water temperature in the central basin increased by an average of 0.037 °C/year between 1983 and 2002 (Burns et al., 2005). If that rate of warming has been consistent, the central basin would have warmed by 1.3 °C between 1983 and 2018, but more significant warming could have occurred if the warming rate has accelerated since 2002. The multi-decadal warming may have factored into the current cyanobacterial blooms in the central basin, and continued warming could lead to more massive blooms or a shift to higher dominance by *Microcystis*.

Hypoxic and anoxic waters and the subsequent release of DRP and reduced Fe is a mechanism that can support cyanobacterial blooms (Funkey et al., 2014; Molot et al., 2014; Verschoor et al., 2017). Lake Erie's central basin has been long known to develop a summertime anoxic hypolimnion (Bertram, 1993; Charlton, 1980; Rosa and Burns, 1987), and the areal extent of the anoxic zone has increased since the mid-1990s (Scavia et al., 2014; Zhou et al., 2013). The July blooms of *Dolichospermum* occurred when the basin was thermally stratified; however, there was no relationship between the timing of bloom formation and hypolimnion DO concentration measured at the time of sampling. For example, during the peak of *Dolichospermum* biovolume in summers 2013 and 2015 the hypolimnion DO concentrations were 1.2 and 7.5 mg/L, respectively. Additionally, continuous data loggers deployed near site Lorain throughout 2017 indicated that surface cyanobacterial biomass was not associated with the onset of hypoxia (ESM Fig. S3) and that hypolimnion DRP and total dissolved Fe were below detection throughout 2017 (ESM Fig. S4). Furthermore, it has been documented that the anoxic area reaches its largest areal extent in August or September (Zhou et al., 2013). Therefore, because *Dolichospermum* blooms occurred before wide-spread central basin anoxia, it is unlikely that *Dolichospermum* benefited from anoxic waters; however, it is unknown if transient boundary layer dissolved oxygen dynamics could play a role due to high sediment oxygen demand (0.75 g $O_2/m_2/d$; Rucinski et al., 2014). Contrary to *Dolichospermum*, central basin *Microcystis* blooms reached highest biomass in September and may have benefited from the anoxic waters.

The competition for light among phytoplankton can shape communities because negatively buoyant phytoplankton sink out of the photic zone and positively buoyant cyanobacteria are more competitive for nutrients in calm, light-limited waters (Huisman et al., 2004; Reynolds et al., 1987). The largest cumulative central basin blooms of June and July 2013 and 2015 corresponded with shallower Secchi disk depths (June–July averages 3.8 and 3.3 m, respectively) than the smaller bloom years of 2014, 2016, and 2017 (annual average 5.9, 6.7, and 5.9 m, respectively). Additionally, the second largest blooms June and July of 2003 and 2012 were associated with less than average Secchi disk depths (Binding et al., 2015). While phytoplankton biomass contributes to Secchi disk depth, Burns et al. (2005) suggested the variation of water clarity in the central basin was not explained by chl *a* or TP concentrations but was more associated with sediment loading from tributaries. Therefore, light-limitation, due to sediment loading, can be a driver of higher biomasses of the positively buoyant *Dolichospermum* in the central basin.

Cyanobacterial blooms are most often associated with eutrophication due to excessive nutrient (P and N) concentrations (Reynolds, 2006); additionally, diazotrophic cyanobacteria are typically associated with waters low in N and high P (i.e., low TN: TP ratios; Smith, 1983). In the central basin, however, *Dolichospermum* blooms were present in July when nitrate concentrations and TN: TP ratios were relatively high (nitrate > 20 μmol/L; TN: TP > 100 by moles) compared to August and September (nitrate < 10 μmol/L; Fig. 8). The presence of

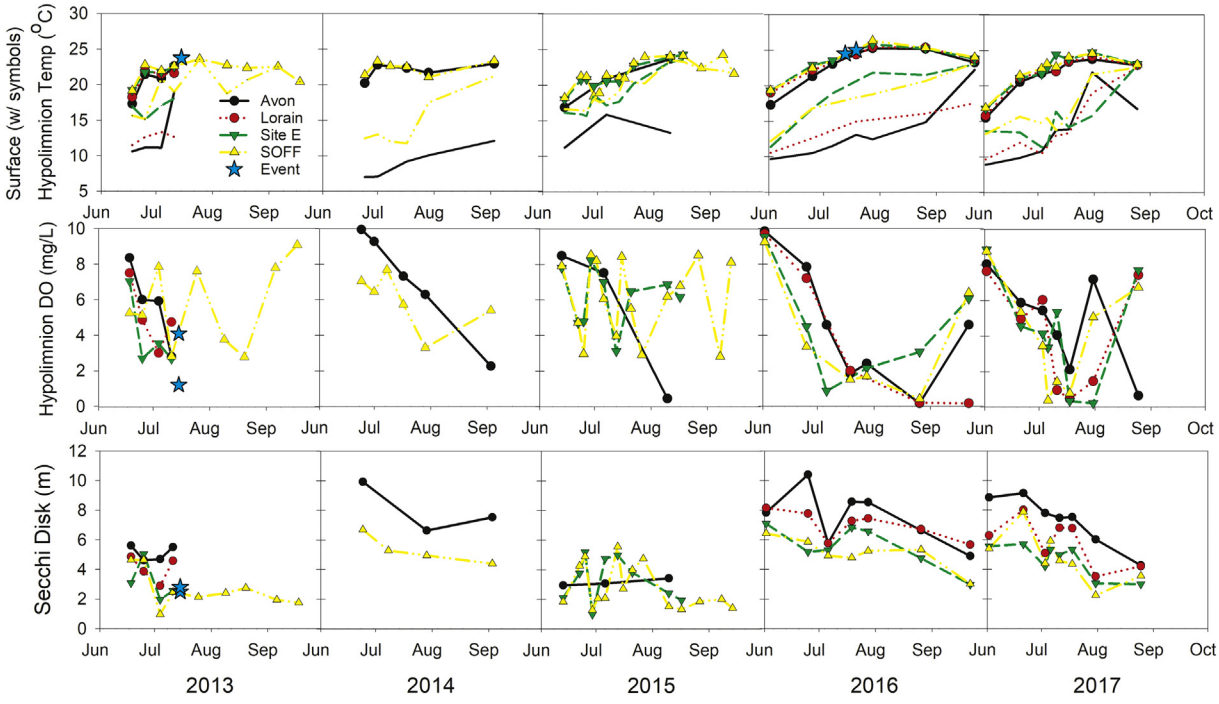

Fig. 7. Water temperature (°C) (top row), hypolimnion dissolved oxygen concentration (mg/L) (middle row), and Secchi disk depth (m) (bottom row) measured at 4 fixed sites (lines) and at event-based locations (stars). In the temperature graph, the lines with symbols represent the temperature measured at 1 m and lines without symbols represent the temperature measured just above the lake bottom. Note that not all sites were sampled in 2013, 2014, and 2015.

Dolichospermum in high N, low P waters is counterintuitive with the general tenet that diazotrophic cyanobacteria are selected for in low N, high P waters (Paerl and Otten, 2016). Nitrate assimilation requires Fe (Flores and Herrero, 2005; Havens et al., 2012); low availability of Fe in the presence of nitrate and the absence of ammonium can lead to a de facto N-limitation because the nitrate is unavailable for assimilation. Fe limitation has been documented in the eastern basin of Lake Erie (North et al., 2007; Twiss et al., 2000) and Lake Superior (Sterner et al., 2004).

Ammonium concentrations were below detection throughout the summer in the epilimnion, but high ammonium concentrations did occur in the hypolimnion (ESM Fig. S4). Buoyancy regulation by *Dolichospermum* would provide access to ammonium in the hypolimnion (Brookes et al., 1999) because the maximum floating and sinking rates for *Dolichospermum* have been reported to range from 0.40 m/h to 2.01 m/h (Brookes et al., 1999; Reynolds et al., 1987; Walsby et al., 1991), which converts to 4.8 m to 24 m over a 12-h period. The central basin hypolimnion would only be accessible to the *Dolichospermum* migrating at the upper half of that reported range. However, *Dolichospermum* would not need to migrate through the entire water column because it would lose buoyancy in little as 2.9 h when exposed to light intensities of just 135 μmol photons/m^2/s (Kinsman et al., 1991). Moreover, Walsby et al. (1991) showed *Dolichospermum* could withstand pressures at a depth equivalent to 40 m (which exceeds the maximum depth of the central basin). These combined results indicate that central basin *Dolichospermum* would be capable of accessing ammonium from the hypolimnion.

Recently, theoretical models linked cyanobacteria dominance to Fe availability (Molot et al., 2014; Orihel et al., 2015; Verschoor et al., 2017). In low nutrient lakes, large colonial cyanobacteria made up a higher percentage of the phytoplankton community when the total dissolved Fe concentration was <0.1 μmol/L (Sorichetti et al., 2014), due to their ability to produce siderophores that aid in Fe-scavenging (Sorichetti et al., 2016). Thus, cyanobacteria are less limited by Fe than their eukaryotic counterparts and are more primed to use a pulse of nutrients (Sorichetti et al., 2014, 2016), but lose this advantage in waters with adequate levels of Fe concentration. Indeed, total dissolved Fe concentrations were below detection (<5 nM) in all surface water samples collected during 2016 and 2017. Additionally, cyanobacteria dominance has been linked to reduced Fe (ferrous Fe^{2+}) because cyanobacteria can migrate down to anoxic waters (Molot et al., 2014; Orihel et al., 2015; Verschoor et al., 2017). While this model has merit for lakes that develop an anoxic hypolimnion, it does not explain the *Dolichospermum* blooms in Lake Erie that occur before the onset of hypoxia.

Cyanotoxins in the central basin

Detections of microcystins in early summer (July) only occurred during the bloom-based event sampling in 2013, which also corresponded to the presence of *Planktothrix*. Detections of microcystins in late summer (August and September) were associated with *Microcystis*. Microcystins and *mcyE* were not detected when *Dolichospermum* was the only colony-forming cyanobacterium detected in the central basin. These results agree with previous research by Ouellette et al. (2006) that showed only *Microcystis* and *Planktothrix* were responsible for the production of microcystins in Lake Erie. Although microcystins are often associated with *Dolichospermum* blooms in other bodies of water (Li et al., 2016), there have been other *Dolichospermum* populations found to be incapable of microcystins synthesis (Capelli et al., 2017; Salmaso et al., 2015). Additionally, when *Microcystis* was present in the central basin in August and September, the concentrations of microcystins (<2 μg/L) were much lower than those reported in the western basin and Sandusky Bay, which are dominated by and have much greater biomasses of *Microcystis* and *Planktothrix*, respectively. Higher concentrations of microcystins could be expected in the central basin if greater biomasses of toxin-producing *Microcystis* were transported from the western basin. However, one should not assume a proportional relationship between cyanobacterial biomass and cyanotoxin concentration (Gobler et al., 2016).

The co-occurrence of the *sxtA* gene and a known saxitoxin-producing cyanobacterium, *Dolichospermum* (Li et al., 2016), suggests

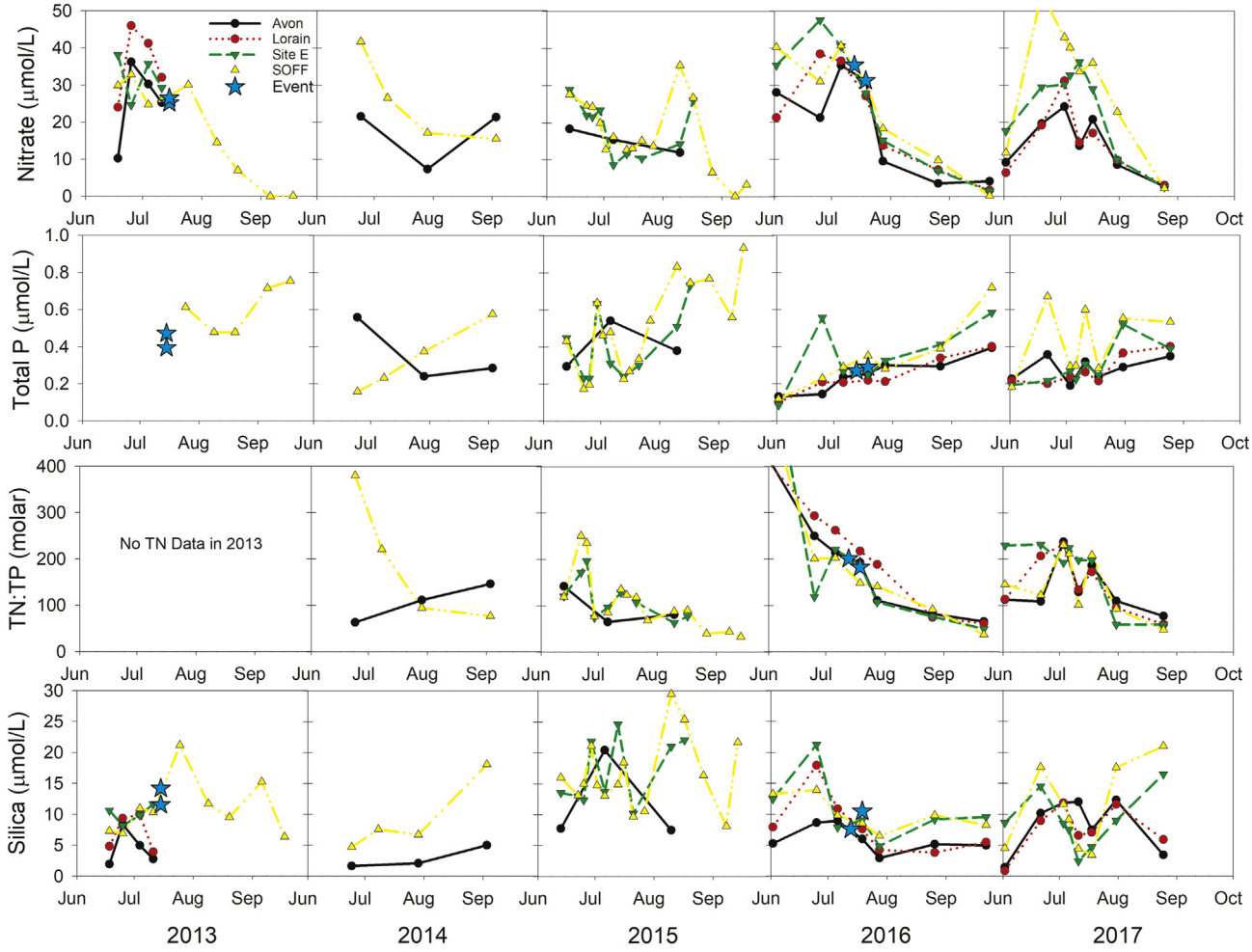

Fig. 8. Nitrate concentrations (µmol/L) (top row), total phosphorus concentrations (µmol/L) (second row), the molar ratio of total nitrogen to total phosphorus concentration (third row) and silicate concentration (µmol/L) (bottom row) measured at 4 fixed sites (lines) and at event-based locations (stars). Note that not all sites were sampled in 2013, 2014, and 2015.

the possibility that saxitoxins could be present in the central basin of Lake Erie during June and July. A survey of Australian lakes with *Dolichospermum* presence reported a positive correlation between *sxtA* gene copies and saxitoxins concentrations measured by high-pressure liquid chromatography (HPLC) and that saxitoxins were not detectable until *sxtA* exceeded 7610 copies/mL (Al-Tebrineh et al., 2010), a *sxtA* level that is an order of magnitude greater than *sxtA* measured in the central basin. Another recent study measured similar levels of *sxtA* in Lake Okeechobee (Florida, USA) during 2016 as the central basin and reported that saxitoxins were not detected by an ELISA method, but suggested that low levels of saxitoxins could have been detected if more advanced methods were used (Kramer et al., 2018). While the numbers of *sxtA* copies we report for the central basin were lower than that reported by studies above, it is important to point out that our samples were integrated throughout the upper 8 m of the water column. It is likely that *Dolichospermum* surface scums would have a much higher number of *sxtA* gene copies and the potential to detect saxitoxins would be greater. Future studies are warranted that measure saxitoxins concentrations and that investigate environmental factors associated with saxitoxins production in the central basin of Lake Erie.

Several Ohio municipalities along the Lake Erie shoreline use the central basin as a source of drinking water. Ohio EPA requires drinking water treatment plants (throughout the state) to analyze their intake lake water weekly for microcystins and biweekly or monthly (based on the frequency of detections) for cyanotoxins genes. The results presented here suggest that the required monitoring for cyanotoxins by central basin water treatment plants is a valuable practice. Additionally, because *Dolichospermum* is a known anatoxin-a producer, investigations to determine anatoxin-a risk to Ohio lakeshore communities are warranted.

To compare the central basin cyanotoxin gene results to other bodies of water in Ohio, the Ohio EPA dataset was accessed for *sxtA* and *mcyE* gene copy data from every drinking water treatment plant in Ohio for years 2016 and 2017 (Ohio E.P.A., 2018). A total of 5111 sample were analyzed during 2016 and 2017. The *sxtA* and *mcyE* genes were detected in 6.7% and 12.7% of all samples, respectively, and furthermore, among the Ohio EPA detections, 81.2% and 70.6% of the samples had a higher number of *sxtA* and *mcyE* gene copies than the highest level of gene copies detected the central basin (304 and 715/mL, respectively; Fig. 6). Additionally, many of the Ohio EPA samples had gene copies that were 2 to 3 orders of magnitude greater than the central basin. These results indicate that *sxtA* and *mcyE* in the offshore waters of Lake Erie's central basin are low when compared to other lakes of Ohio. However, the offshore blooms can wash ashore and concentrate on beaches, which happened at Fairport Harbor in July 2016 (and triggered an event sampling).

Mitigation of central basin blooms

Eutrophication of Lake Erie in the mid-1900s was reversed by reducing P loading into the lake primarily via point source regulation enacted following the Great Lakes Water Quality Agreement (GLWQA) in 1972 (DePinto et al., 1986). Since the mid-1990s, however, the lake is again experiencing re-eutrophication (Kane et al., 2015; Matisoff and Ciborowski, 2005; Steffen et al., 2014), and the GLWQA was updated in 2012 to address the western basin *Microcystis* blooms, central basin

hypoxia, and eastern basin *Cladophora*. The Annex 4 committee of the 2012 GLWQA set P load reduction targets of 40% (Scavia et al., 2016). One can ask the question: Will the P load reduction also mitigate the central basin blooms? Because the presence of *Dolichospermum* in the central basin and other relatively nutrient-poor waters (Callieri et al., 2014; Carey et al., 2008; Salmaso et al., 2015; Winter et al., 2014) could be the result of an interaction of several environmental factors (as discussed above), it remains unclear how P load reductions will affect *Dolichospermum* during early summer. Conversely, late summer central basin *Microcystis* blooms are an extension of the western basin bloom. Therefore, because P load reduction will reduce *Microcystis* biomass in the western basin (Scavia et al., 2016), P load reduction will also reduce central basins *Microcystis* biomass. Additionally, dual nutrient (P and N) management has been suggested as a required means to control eutrophication (Conley et al., 2009; Paerl et al., 2016b) and specifically for the western basin of Lake Erie and Sandusky Bay (Gobler et al., 2016). It is unclear how a P-only approach versus a dual nutrient approach will affect the central basin *Dolichospermum* blooms. Finally, because larger biomasses of *Dolichospermum* were observed in summers with reduced water clarity, lake managers should consider minimizing sediment loads into the central basin in addition to nutrient load reduction.

Conclusion

Dolichospermum blooms occurred in the central basin of Lake Erie before the onset of the western basin *Microcystis* blooms indicating that separate environmental factors affect the central basin bloom dynamics. It is likely that an interaction between temperature, low bioavailabilities of Fe and N, and light-limited waters selected for *Dolichospermum* (over other cyanobacteria) in July and then selected for *Microcystis* in August and September. Larger *Dolichospermum* bloom years were associated with reduced water clarity, and therefore, mitigation strategies should incorporate erosion control and sediment load reductions. The *sxtA* gene was present when *Dolichospermum* dominated the cyanobacterial community, and future research is needed to determine if *Dolichospermum* blooms are producing saxitoxins in the central basin. To ensure public safety, it is recommended that coastal central basin communities continue to monitor for the *sxtA* and *mcyE* genes. Finally, the more recent years (since 2011), Lake Erie's central basin has had the largest early summer (*Dolichospermum*) and late summer (*Microcystis*) cyanobacterial blooms, indicating that eutrophication and cyanobacterial blooms are not just a western basin problem.

Acknowledgments

This work was supported by a Harmful Algal Bloom Research Initiative grant from the Ohio Department of Higher Education, Ohio Sea Grant (NA14OAR4170067), and the Ohio EPA (OSUSL-FDNear10). We thank Sam McCoy, Brianna Zellner, Kat Rossos, Callie Nauman, Chris Boehler for laboratory assistance and the many Stone Lab seasonal staff and students who assisted in sample collection throughout the project. We thank the Maritime Archaeology Survey Team for deploying water quality sondes at the Morning Star shipwreck site off Lorain. We thank Heather Raymond and Scott Winkler from Ohio EPA for helpful discussions. We also thank three anonymous reviewers who helped improve the manuscript.

Appendix A. Supplementary data

Supplementary data to this article can be found online at https://doi.org/10.1016/j.jglr.2018.12.006.

References

Al-Tebrineh, J., Mihali, T.K., Pomati, F., Neilan, B.A., 2010. Detection of saxitoxin-producing cyanobacteria and *Anabaena circinalis* in environmental water blooms by quantitative PCR. Appl. Environ. Microbiol. 76, 7836–7842. https://doi.org/10.1128/AEM.00174-10.

Al-Tebrineh, J., Pearson, L.A., Yasar, S.A., Neilan, B.A., 2012. A multiplex qPCR targeting hepato- and neurotoxigenic cyanobacteria of global significance. Harmful Algae 15, 19–25. https://doi.org/10.1016/j.hal.2011.11.001.

Bertram, P.E., 1993. Total phosphorus and dissolved oxygen trends in the central basin of Lake Erie, 1970–1991. J. Great Lakes Res. 19, 224–236. https://doi.org/10.1016/S0380-1330(93)71213-7.

Binding, C.E., Greenberg, T.A., Watson, S.B., Rastin, S., Gould, J., 2015. Long term water clarity changes in North America's Great Lakes from multi-sensor satellite observations. Limnol. Oceanogr. 60, 1976–1995. https://doi.org/10.1002/lno.10146.

Blomqvist, P., Petterson, A., Hyenstrand, P., 1994. Ammonium-nitrogen: a key regulatory factor causing dominance of non-nitrogen-fixing cyanobacteria in aquatic systems. Arch. Für Hydrobiol. 132, 141–164.

Bolsenga, S.J., Herdendorf, C.E., 1993. Lake Erie and Lake Saint Clair Handbook. Wayne State University Press.

Bridgeman, T.B., Penamon, W.A., 2010. *Lyngbya wollei* in western Lake Erie. J. Great Lakes Res. 36, 167–171.

Bridgeman, T.B., Schloesser, D.W., Krause, A.E., 2006. Recruitment of *Hexagenia* mayfly nymphs in western Lake Erie linked to environmental variability. Ecol. Appl. 16, 601–611.

Brookes, J.D., Ganf, G.G., Green, D., Whittington, J., 1999. The influence of light and nutrients on buoyancy, filament aggregation and flotation of *Anabaena circinalis*. J. Plankton Res. 21, 327–341. https://doi.org/10.1093/plankt/21.2.327.

Burns, N.M., Rockwell, D.C., Bertram, P.E., Dolan, D.M., Ciborowski, J.J.H., 2005. Trends in temperature, Secchi depth, and dissolved oxygen depletion rates in the central basin of Lake Erie, 1983–2002. J. Great Lakes Res. 31, 35–49. https://doi.org/10.1016/S0380-1330(05)70303-8 Lake Erie Trophic Status Collaborative Study.

Callieri, C., Bertoni, R., Contesini, M., Bertoni, F., 2014. Lake level fluctuations boost toxic cyanobacterial "oligotrophic blooms". PLoS One 9, e109526. https://doi.org/10.1371/journal.pone.0109526.

Capelli, C., Ballot, A., Cerasino, L., Papini, A., Salmaso, N., 2017. Biogeography of bloom-forming microcystin producing and non-toxigenic populations of *Dolichospermum lemmermannii* (Cyanobacteria). Harmful Algae 67, 1–12. https://doi.org/10.1016/j.hal.2017.05.004.

Carey, C.C., Weathers, K.C., Cottingham, K.L., 2008. *Gloeotrichia echinulata* blooms in an oligotrophic lake: helpful insights from eutrophic lakes. J. Plankton Res. 30, 893–904. https://doi.org/10.1093/plankt/fbn055.

Chaffin, J.D., Bridgeman, T.B., Bade, D.L., 2013. Nitrogen constrains the growth of late summer cyanobacterial blooms in Lake Erie. Adv. Microbiol. 03, 16–26. https://doi.org/10.4236/aim.2013.36A003.

Chaffin, J.D., Sigler, V., Bridgeman, T.B., 2014. Connecting the blooms: tracking and establishing the origin of the record-breaking Lake Erie *Microcystis* bloom of 2011 using DGGE. Aquat. Microb. Ecol. 73, 29–39.

Chaffin, J.D., Davis, T.W., Smith, D.J., Baer, M.M., Dick, G.J., 2018. Interactions between nitrogen form, loading rate, and light intensity on *Microcystis* and *Planktothrix* growth and microcystin production. Harmful Algae 73, 84–97. https://doi.org/10.1016/j.hal.2018.02.001.

Chapra, S.C., Robertson, A., 1977. Great Lakes eutrophication: the effect of point source control of total phosphorus. Science 196, 1448. https://doi.org/10.1126/science.196.4297.1448.

Charlton, M.N., 1980. Oxygen depletion in Lake Erie: has there been any change? Can. J. Fish. Aquat. Sci. 37, 72–80. https://doi.org/10.1139/f80-007.

Chia, M.A., Jankowiak, J.G., Kramer, B.J., Goleski, J.A., Huang, I.-S., Zimba, P.V., do Carmo Bittencourt-Oliveira, M., Gobler, C.J., 2018. Succession and toxicity of *Microcystis* and *Anabaena* (*Dolichospermum*) blooms are controlled by nutrient-dependent allelopathic interactions. Harmful Algae 74, 67–77. https://doi.org/10.1016/j.hal.2018.03.002.

Conley, D.J., Paerl, H.W., Howarth, R.W., Boesch, D.F., Seitzinger, S.P., Havens, K.E., Lancelot, C., Likens, G.E., 2009. Controlling eutrophication: nitrogen and phosphorus. Science 323, 1014–1015. https://doi.org/10.1126/science.1167755.

Conroy, J.D., Kane, D.D., Dolan, D.M., Edwards, W.J., Charlton, M.N., Culver, D.A., 2005. Temporal trends in Lake Erie plankton biomass: roles of external phosphorus loading and dreissenid mussels. J. Great Lakes Res. Supplement 2, 89–110. https://doi.org/10.1016/S0380-1330(05)70307-5 Lake Erie Trophic Status Collaborative Study 31.

Conroy, J.D., Kane, D.D., Quinlan, E.L., Edwards, W.J., Culver, D.A., 2017. Abiotic and biotic controls of phytoplankton biomass dynamics in a freshwater tributary, estuary, and large lake ecosystem: Sandusky Bay (Lake Erie) chemostat. Inland Waters 7, 1–20. https://doi.org/10.1080/20442041.2017.1395142.

Davis, C.C., 1964. Evidence for the eutrophication of Lake Erie from phytoplankton records. Limnol. Oceanogr. 9, 275–283.

Davis, T.W., Bullerjahn, G.S., Tuttle, T., McKay, R.M., Watson, S.B., 2015. Effects of increasing nitrogen and phosphorus concentrations on phytoplankton community growth and toxicity during *Planktothrix* blooms in Sandusky Bay, Lake Erie. Environ. Sci. Technol. 49, 7197–7207.

Davis, T.W., Stumpf, R.P., Bullerjahn, G.S., McKay, R.M.L., Chaffin, J.D., Bridgeman, T.B., Winslow, C., 2019. Science meets policy: A framework for determining impairment designation criteria for large waterbodies affected by cyanobacterial harmful algal blooms. Harmful Algae 81, 59–64.

DePinto, J.V., Young, T.C., McIlroy, L.M., 1986. Great Lakes water quality improvement. Environ. Sci. Technol. 20, 752–759.

Flores, E., Herrero, A., 2005. Nitrogen assimilation and nitrogen control in cyanobacteria. Biochem. Soc. Trans. 33, 164–167. https://doi.org/10.1042/BST0330164.

Funkey, C.P., Conley, D.J., Reuss, N.S., Humborg, C., Jilbert, T., Slomp, C.P., 2014. Hypoxia sustains cyanobacteria blooms in the Baltic Sea. Environ. Sci. Technol. 48, 2598–2602. https://doi.org/10.1021/es404395a.

GDAL/OGR contributors, 2018. GDAL/OGR Geospatial Data Abstraction software Library. Open Source Geospatial Foundation website. https://gdal.org.
Gobler, C.J., Burkholder, J.M., Davis, T.W., Harke, M.J., Johengen, T., Stow, C.A., Van de Waal, D.B., 2016. The dual role of nitrogen supply in controlling the growth and toxicity of cyanobacterial blooms. Harmful Algae 54, 87–97. https://doi.org/10.1016/j.hal.2016.01.010 Global Expansion of Harmful Cyanobacterial Blooms: Diversity, ecology, causes, and controls.
Golnick, P.C., Chaffin, J.D., Bridgeman, T.B., Zellner, B.C., Simons, V.E., 2016. A comparison of water sampling and analytical methods in western Lake Erie. J. Great Lakes Res. 42, 965–971. https://doi.org/10.1016/j.jglr.2016.07.031.
Havens, S.M., Hassler, C.S., North, R.L., Guildford, S.J., Silsbe, G., Wilhelm, S.W., Twiss, M.R., 2012. Iron plays a role in nitrate drawdown by phytoplankton in Lake Erie surface waters as observed in lake-wide assessments. Can. J. Fish. Aquat. Sci. 69, 369–381. https://doi.org/10.1139/f2011-157.
Herdendorf, C.E., 1982. Large lakes of the world. J. Great Lakes Res. 8, 379–412. https://doi.org/10.1016/S0380-1330(82)71982-3.
Huisman, J., Sharples, J., Stroom, J.M., Visser, P.M., Kardinaal, W.E.A., Verspagen, J.M.H., Sommeijer, B., 2004. Changes in turbulent mixing shift competition for light between phytoplankton species. Ecology 85, 2960–2970. https://doi.org/10.1890/03-0763.
Kane, D.D., Conroy, J.D., Richards, R.P., Baker, D.B., Culver, D.A., 2014. Re-eutrophication of Lake Erie: correlations between tributary nutrient loads and phytoplankton biomass. J. Great Lakes Res. 40, 496–501.
Kane, D.D., Ludsin, S.A., Briland, R.D., Culver, D.A., Munawar, M., 2015. Ten+ years gone: continued degradation of offshore planktonic communities in US waters of Lake Erie's western and central basins (2003−2013). J. Great Lakes Res. 41, 930–933.
Kinsman, R., Ibelings, B.W., Walsby, A.E., 1991. Gas vesicle collapse by turgor pressure and its role in buoyancy regulation by *Anabaena flos-aquae*. Microbiology 137, 1171–1178. https://doi.org/10.1099/00221287-137-5-1171.
Kramer, B.J., Davis, T.W., Meyer, K.A., Rosen, B.H., Goleski, J.A., Dick, G.J., Oh, G., Gobler, C.J., 2018. Nitrogen limitation, toxin synthesis potential, and toxicity of cyanobacterial populations in Lake Okeechobee and the St. Lucie River Estuary, Florida, during the 2016 state of emergency event. PLoS One 13, e0196278. https://doi.org/10.1371/journal. pone.0196278.
Lewis, W.M., Wurtsbaugh, W.A., 2008. Control of lacustrine phytoplankton by nutrients: erosion of the phosphorus paradigm. Int. Rev. Hydrobiol. 93, 446–465. https://doi.org/10.1002/iroh.200811065.
Li, X., Dreher, T.W., Li, R., 2016. An overview of diversity, occurrence, genetics and toxin production of bloom-forming *Dolichospermum* (*Anabaena*) species. Harmful Algae 54, 54–68. https://doi.org/10.1016/j.hal.2015.10.015 Global Expansion of Harmful Cyanobacterial Blooms: Diversity, ecology, causes, and controls.
Ludsin, S.A., Kershner, M.W., Blocksom, K.A., Knight, R.L., Stein, R.A., 2001. Life after death in Lake Erie: nutrient controls drive fish species richness, rehabilitation. Ecol. Appl. 11, 731–746. https://doi.org/10.1890/1051-0761(2001)011[0731:LADILE]2.0.CO;2.
Lunetta, R.S., Schaeffer, B.A., Stumpf, R.P., Keith, D., Jacobs, S.A., Murphy, M.S., 2015. Evaluation of cyanobacteria cell count detection derived from MERIS imagery across the eastern USA. Remote Sens. Environ. 157, 24–34. https://doi.org/10.1016/j.rse.2014.06.008 Special Issue: Remote Sensing of Inland Waters.
Makarewicz, J.C., 1993. Phytoplankton biomass and species composition in Lake Erie, 1970 to 1987. J. Great Lakes Res. 19, 258–274.
Matisoff, G., Ciborowski, J.J.H., 2005. Lake Erie trophic status collaborative study. J. Great Lakes Res. 31, 1–10.
Molot, L.A..A., Watson, S.B..B., Creed, I.F..F., Trick, C.G..G., McCabe, S.K..K., Verschoor, M.J..J., Sorichetti, R.J..J., Powe, C., Venkiteswaran, J.J..J., Schiff, S.L..L., 2014. A novel model for cyanobacteria bloom formation: the critical role of anoxia and ferrous iron. Freshw. Biol. https://doi.org/10.1111/fwb.12334 n/a.
North, R.L., Guildford, S.J., Smith, R.E.H., Havens, S.M., Twiss, M.R., 2007. Evidence for phosphorus, nitrogen, and iron colimitation of phytoplankton communities in Lake Erie. Limnol. Oceanogr. 52, 315–328. https://doi.org/10.4319/lo.2007.52.1.0315.
Ohio E.P.A., 2018. Harmful Algal Blooms (HAB) information for public water systems. Website. http://www.epa.ohio.gov/ddagw/hab, Accessed date: 31 August 2018.
O'Neil, J.M., Davis, T.W., Burford, M.A., Gobler, C.J., 2012. The rise of harmful cyanobacteria blooms: the potential roles of eutrophication and climate change. Harmful Algae 14, 313–334. https://doi.org/10.1016/j.hal.2011.10.027 Harmful Algae—The requirement for species-specific information.
Orihel, D.M., Schindler, D.W., Ballard, N.C., Graham, M.D., O'Connell, D.W., Wilson, L.R., Vinebrooke, R.D., 2015. The nutrient pump: Iron-poor sediments fuel low nitrogen-to-phosphorus ratios and cyanobacterial blooms in polymictic lakes. Limnol. Oceanogr. 60, 856–871.
Ouellette, A.J., Handy, S.M., Wilhelm, S.W., 2006. Toxic *Microcystis* is widespread in Lake Erie: PCR detection of toxin genes and molecular characterization of associated cyanobacterial communities. Microb. Ecol. 51, 154–165.
Paerl, H.W., Huisman, J., 2008. Blooms like it hot. Science 320, 57–58. https://doi.org/10.1126/science.1155398.
Paerl, H.W., Otten, T.G., 2016. Dueling" CyanoHABs": unraveling the environmental drivers controlling dominance and succession among diazotrophic and non-N2-fixing harmful cyanobacteria. Environ. Microbiol. 18, 316–324.
Paerl, H.W., Xu, H., McCarthy, M.J., Zhu, G., Qin, B., Li, Y., Gardner, W.S., 2011. Controlling harmful cyanobacterial blooms in a hyper-eutrophic lake (Lake Taihu, China): the need for a dual nutrient (N & P) management strategy. Water Res. 45, 1973–1983. https://doi.org/10.1016/j.watres.2010.09.018.
Paerl, H.W., Gardner, W.S., Havens, K.E., Joyner, A.R., McCarthy, M.J., Newell, S.E., Qin, B., Scott, J.T., 2016a. Mitigating cyanobacterial harmful algal blooms in aquatic ecosystems impacted by climate change and anthropogenic nutrients. Harmful Algae 54, 213–222. https://doi.org/10.1016/j.hal.2015.09.009 Global Expansion of Harmful Cyanobacterial Blooms: Diversity, ecology, causes, and controls.
Paerl, H.W., Scott, J.T., McCarthy, M.J., Newell, S.E., Gardner, W.S., Havens, K.E., Hoffman, D.K., Wilhelm, S.W., Wurtsbaugh, W.A., 2016b. It takes two to tango: when and where dual nutrient (N & P) reductions are needed to protect lakes and downstream ecosystems. Environ. Sci. Technol. 50, 10805–10813. https://doi.org/10.1021/acs.est.6b02575.
Qian, S.S., Chaffin, J.D., DuFour, M.R., Sherman, J.J., Golnick, P.C., Collier, C.D., Nummer, S.A., Margida, M.G., 2015. Quantifying and reducing uncertainty in estimated microcystin concentrations from the ELISA method. Environ. Sci. Technol. 49, 14221–14229. https://doi.org/10.1021/acs.est.5b03029.
Reavie, E.D., Barbiero, R.P., Allinger, L.E., Warren, G.J., 2014. Phytoplankton trends in the Great Lakes, 2001–2011. J. Great Lakes Res. 40, 618–639.
Reynolds, C.S., 2006. Ecology of Phytoplankton. Cambridge University Press.
Reynolds, C.S., Oliver, R.L., Walsby, A.E., 1987. Cyanobacterial dominance: the role of buoyancy regulation in dynamic lake environments. N. Z. J. Mar. Freshw. Res. 21, 379–390.
Rosa, F., Burns, N.M., 1987. Lake Erie central basin oxygen depletion changes from 1929–1980. J. Great Lake Res. 13, 684–696. https://doi.org/10.1016/S0380-1330(87)71683-9 Lake Erie Binational Study.
Rucinski, D.K., DePinto, J.V., Scavia, D., Beletsky, D., 2014. Modeling Lake Erie's hypoxia response to nutrient loads and physical variability. J. Great Lakes Res. 40, 151–161. https://doi.org/10.1016/j.jglr.2014.02.003 Current state and future perspectives of environmental modeling in the Great Lakes.
Salmaso, N., Capelli, C., Shams, S., Cerasino, L., 2015. Expansion of bloom-forming *Dolichospermum lemmermannii* (Nostocales, Cyanobacteria) to the deep lakes south of the Alps: colonization patterns, driving forces and implications for water use. Harmful Algae 50, 76–87.
Scavia, D., David Allan, J., Arend, K.K., Bartell, S., Beletsky, D., Bosch, N.S., Brandt, S.B., Briland, R.D., Daloğlu, I., DePinto, J.V., Dolan, D.M., Evans, M.A., Farmer, T.M., Goto, D., Han, H., Höök, T.O., Knight, R., Ludsin, S.A., Mason, D., Michalak, A.M., Peter Richards, R., Roberts, J.J., Rucinski, D.K., Rutherford, E., Schwab, D.J., Sesterhenn, T.M., Zhang, H., Zhou, Y., 2014. Assessing and addressing the re-eutrophication of Lake Erie: central basin hypoxia. J. Great Lakes Res. 40, 226–246. https://doi.org/10.1016/j.jglr.2014.02.004.
Scavia, D., DePinto, J.V., Bertani, I., 2016. A multi-model approach to evaluating target phosphorus loads for Lake Erie. J. Great Lakes Res. 42, 1139–1150. https://doi.org/10.1016/j.jglr.2016.09.007.
Schindler, D.W., 1977. Evolution of phosphorus limitation in lakes. Science 195, 260–262. https://doi.org/10.1126/science.195.4275.260.
Schindler, D.W., Carpenter, S.R., Chapra, S.C., Hecky, R.E., Orihel, D.M., 2016. Reducing phosphorus to curb lake eutrophication is a success. Environ. Sci. Technol. 50, 8923–8929. https://doi.org/10.1021/acs.est.6b02204.
Smith, V.H., 1983. Low nitrogen to phosphorus ratios favor dominance by blue-green algae in lake phytoplankton. Science 221, 669–671.
Snodgrass, W.J., 1987. Analysis of models and measurements for sediment oxygen demand in Lake Erie. J. Great Lakes Res. 13, 738–756.
Sorichetti, R.J., Creed, I.F., Trick, C.G., 2014. Evidence for iron-regulated cyanobacterial predominance in oligotrophic lakes. Freshw. Biol. 59, 679–691.
Sorichetti, R.J., Creed, I.F., Trick, C.G., 2016. Iron and iron-binding ligands as cofactors that limit cyanobacterial biomass across a lake trophic gradient. Freshw. Biol. 61, 146–157. https://doi.org/10.1111/fwb.12689.
Steffen, M.M., Belisle, B.S., Watson, S.B., Boyer, G.L., Wilhelm, S.W., et al., 2014. Status, causes and controls of cyanobacterial blooms in Lake Erie. J. Great Lakes Res. 40, 215–225.
Steffen, M.M., Davis, T.W., McKay, R.M.L., Bullerjahn, G.S., Krausfeldt, L.E., Stough, J.M.A., Neitzey, M.L., Gilbert, N.E., Boyer, G.L., Johengen, T.H., Gossiaux, D.C., Burtner, A.M., Palladino, D., Rowe, M.D., Dick, G.J., Meyer, K.A., Levy, S., Boone, B.E., Stumpf, R.P., Wynne, T.T., Zimba, P.V., Gutierrez, D., Wilhelm, S.W., 2017. Ecophysiological examination of the Lake Erie *Microcystis* bloom in 2014: linkages between biology and the water supply shutdown of Toledo, OH. Environ. Sci. Technol. 51, 6745–6755. https://doi.org/10.1021/acs.est.7b00856.
Sterner, R.W., Smutka, T.M., McKay, R.M.L., Xiaoming, Q., Brown, E.T., Sherrell, R.M., 2004. Phosphorus and trace metal limitation of algae and bacteria in Lake Superior. Limnol. Oceanogr. 49, 495–507.
Stumpf, R.P., Wynne, T.T., Baker, D.B., Fahnenstiel, G.L., 2012. Interannual variability of cyanobacterial blooms in Lake Erie. PLoS One 7, e42444.
Stumpf, R.P., Johnson, L.T., Wynne, T.T., Baker, D.B., 2016. Forecasting annual cyanobacterial bloom biomass to inform management decisions in Lake Erie. J. Great Lakes Res. 42, 1174–1183. https://doi.org/10.1016/j.jglr.2016.08.006.
Twiss, M.R., Auclair, J.C., Charlton, M.N., 2000. An investigation into iron-stimulated phytoplankton productivity in epipelagic Lake Erie during thermal stratification using trace metal clean techniques. Can. J. Fish. Aquat. Sci. 57, 86–95.
Verschoor, M.J., Powe, C.R., McQuay, E., Schiff, S.L., Venkiteswaran, J.J., Li, J., Molot, L.A., 2017. Internal iron loading and warm temperatures are preconditions for cyanobacterial dominance in embayments along Georgian Bay, Great Lakes. Can. J. Fish. Aquat. Sci. 74, 1439–1453. https://doi.org/10.1139/cjfas-2016-0377.
Visser, P.M., Verspagen, J.M.H., Sandrini, G., Stal, L.J., Matthijs, H.C.P., Davis, T.W., Paerl, H.W., Huisman, J., 2016. How rising CO_2 and global warming may stimulate harmful cyanobacterial blooms. Harmful Algae 54, 145–159. https://doi.org/10.1016/j.hal.2015.12.006 Global Expansion of Harmful Cyanobacterial Blooms: Diversity, ecology, causes, and controls.
Walsby, A.E., Kinsman, R., Ibelings, B.W., Reynolds, C.S., 1991. Highly buoyant colonies of the cyanobacterium *Anabaena lemmermannii* form persistent surface waterblooms. Arch. Für Hydrobiol. 121, 261–280.
Watson, S.B., Miller, C., Arhonditsis, G., Boyer, G.L., Carmichael, W., Charlton, M.N., Confesor, R., Depew, D.C., Höök, T.O., Ludsin, S.A., Matisoff, G., McElmurry, S.P., Murray, M.W., Peter Richards, R., Rao, Y.R., Steffen, M.M., Wilhelm, S.W., 2016. The

re-eutrophication of Lake Erie: harmful algal blooms and hypoxia. Harmful Algae 56, 44–66. https://doi.org/10.1016/j.hal.2016.04.010.
Wellburn, A.R., 1994. The spectral determination of chlorophyll *a* and chlorophyll *b*, as well as total carotenoids, using various solvents with spectrophotometers of different resolution. J. Plant Physiol. 144, 307–313.
Winter, J.G., Palmer, M.E., Howell, E.T., Young, J.D., 2014. Long term changes in nutrients, chloride, and phytoplankton density in the nearshore waters of Lake Erie. J. Great Lakes Res.
Wynne, T.T., Stumpf, R.P., 2015. Spatial and temporal patterns in the seasonal distribution of toxic cyanobacteria in western Lake Erie from 2002–2014. Toxins 7, 1649–1663.
Wynne, T.T., Stumpf, R.P., Tomlinson, M.C., Warner, R.A., Tester, P.A., Dyble, J., Fahnenstiel, G.L., 2008. Relating spectral shape to cyanobacterial blooms in the Laurentian Great Lakes. Int. J. Remote Sens. 29, 3665–3672.
Wynne, T.T., Stumpf, R.P., Briggs, T.O., 2013. Comparing MODIS and MERIS spectral shapes for cyanobacterial bloom detection. Int. J. Remote Sens. 34, 6668–6678. https://doi.org/10.1080/01431161.2013.804228.
Zapomělová, E., Řeháková, K., Jezberová, J., Komárková, J., 2010. Polyphasic characterization of eight planktonic *Anabaena* strains (Cyanobacteria) with reference to the variability of 61 *Anabaena* populations observed in the field. Hydrobiologia 639, 99–113.
Zhou, Y., Obenour, D.R., Scavia, D., Johengen, T.H., Michalak, A.M., 2013. Spatial and temporal trends in Lake Erie hypoxia, 1987–2007. Environ. Sci. Technol. 47, 899–905. https://doi.org/10.1021/es303401b.